Dynamics of structural phase transitions in $(CH_3NH_3)_2CdCl_4$-type compounds

R. Kind
Laboratory of Solid State Physics, Swiss Federal Institute of Technology, Hönggerberg, CH-8093 Zürich, Switzerland

R. Blinc
J. Stefan Institute, University of Ljubljana, Ljubljana, Yugoslavia

B. Žekš
Institute of Biophysics, Faculty of Medicine, and J. Stefan Institute, University of Ljubljana, Ljubljana, Yugoslavia

(Received 7 July 1978)

The dynamical properties of a model describing the structural phase transitions in $(CH_3NH_3)_2CdCl_4$ perovskite-type layer compounds as orientional order-disorder transitions of the CH_3NH_3 groups, are investigated. It is shown that the soft order-parameter-fluctuation modes observed in the low-frequency Raman spectra of $(CH_3NH_3)_2CdCl_4$ and $(CH_3NH_3)_2MnCl_4$, can be understood on the basis of the same model used to explain the static properties of these systems. The nonlinear coupling of the motion of the CH_3NH_3 groups among four equilibrium sites with the $CdCl_4$ octahedral matrix is not essential in the high-temperature phases, but is necessary to describe the monoclinic ground state. The planewise antiphase motion of the CH_3NH_3 groups is included in the model to explain the observed Γ_2^+ mode of the orthorhombic room-temperature phase and the Γ_4^+ mode of the tetragonal low-temperature phase. If the interlayer coupling is assumed to be much weaker than the intralayer one, similar fluctuation frequencies are obtained for the planewise antiphase modes as for the "planewise in phase" modes corresponding to the condensing order-parameter modes of the four-site model.

I. INTRODUCTION

The structural phase transitions in the perovskite-type layer compounds $(CH_3NH_3)_2CdCl_4$ and $(CH_3NH_3)_2MnCl_4$ have their origin in the order-disorder transitions of the basic reorientable units—i.e., the CH_3NH_3 groups—each of which moves among four possible equilibrium positions.[1–10] It was shown that a simple model accounting for all known microscopic details is capable of describing the observed phases in the correct sequence and with the proper transition temperatures.[11] The above two compounds exhibit the same unusual phase sequence,[2–5,12,13] i.e., Table I.

TABLE I. Transition temperature phase sequence of $(CH_3NH_3)_2CdCl_4$ and $(CH_3NH_3)_2MnCl_4$.

	$I4/mmm$	continuous	$Cmca$	discont.	$P4_2/ncm$	discont.	$P2_1/b$
	tetragonal high temperature		orthorhombic room temperature		tetragonal low temperature		monoclinic low temperature
	$Z=1$		$Z=2$		$Z=4$		$Z=2$
$(CH_3NH_3)_2CdCl_4$		484 K		279 K		163 K	
$(CH_3NH_3)_2MnCl_4$		394 K		257 K		94 K	

©1979 The American Physical Society

The number of formula units Z is given for the primitive unit cells. The phase transitions have been investigated in the past by several experimental techniques,[1-10,12-15] and the knowledge of the microscopic details is almost complete.

The structure consists of infinite sheets of corner-sharing MCl_6 octahedra. Such an arrangement closely resembles a plane of the perovskite structure with the metallic ions (Cd,Mn) occupying the B sites in the centers of the octahedra, whereas the A sites in the cavities between the octahedra are occupied by the NH_3 groups of the methylammonium ions (Fig. 1). The NH_3 groups are attached to the chlorine matrix by weak hydrogen bonds, accounting for the four potential wells corresponding to the different orientations of the $CH_3NH_3^+$ ions. The four possible N–C directions of each CH_3NH_3 group are shown schematically in Fig. 1. Interlayer bonding is achieved by long-range Coulomb forces[16] and by Van der Waals forces acting between the CH_3 groups of adjacent layers. A more extensive description of the microscopic details which have been important in deriving the model Hamiltonian is given in Ref. 11.

The tetragonal high-temperature (THT), orthorhombic room temperature (ORT), and tetragonal low-temperature (TLT) phases are characterized by a dynamic disorder of the CH_3NH_3 groups between four potential wells which can be described by the site-occupation probabilities $n_\alpha(\alpha=1,2,3,4)$.

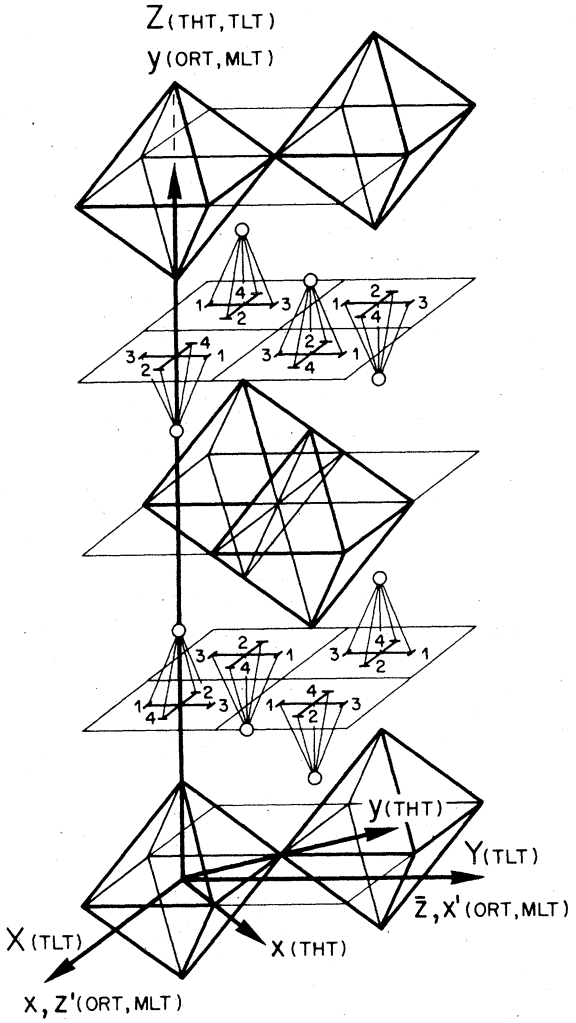

FIG. 1. Structure of $(CH_3NH_3)_2CdCl_4$ in the disordered tetragonal high-temperature (THT) phase. The Cl^- ions are situated at the corners of the octahedra. The Cd^{2+} in the centers of the octahedra are not shown. The $CH_3NH_3^+$ groups are shown schematically by the four possible N–C directions α which are assigned by the numbers 1,2,3,4. The small circles indicate the average N positions.

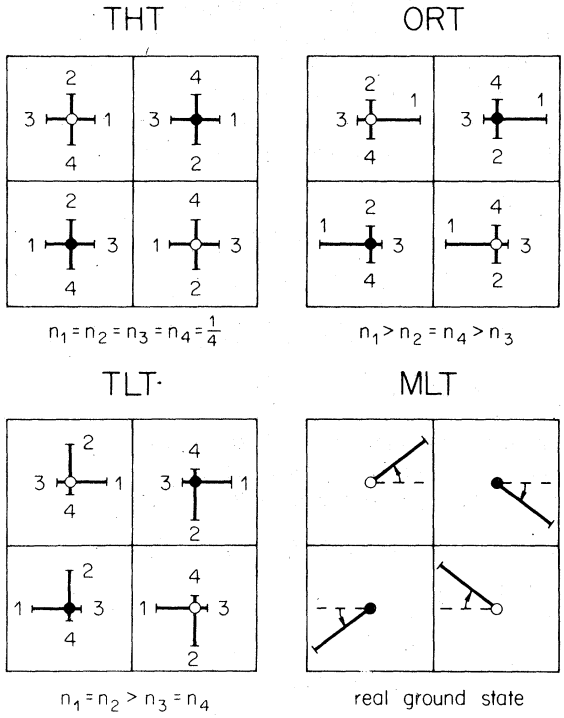

FIG. 2. Schematic representation of the four phases of $(CH_3NH_3)_2CdCl_4$ in the largest primitive unit cell of the system (TLT phase: $Z=4$). The N–C directions of the four CH_3NH_3 groups between two adjacent layers are projected along the Z direction (see Fig. 1). The groups with closed circles are attached to cavities in the upper layer and the ones with open circles to cavities in the lower layer. The assignment of the four different orinetations α of the groups ($\alpha=1,2,3,4$) is chosen in such a way that the probabilities n_α—which are represented by the length of the bars—do not depend on the site of the group in the unit cell for all the phases.

Although there are up to eight CH_3NH_3 groups in the primitive unit cell of the various phases, it is possible to assign the orientations α of all of them in such a way that all phases can be described by the probabilities n_α of one CH_3NH_3 group only (see Figs. 1 and 2) as follows:

THT, $n_1=n_2=n_3=n_4=\frac{1}{4}$,

ORT, $n_1>n_2=n_4>n_3$,

TLT, $n_1=n_2>n_3=n_4$,

The monoclinic low-temperature (MLT) phase cannot be described in terms of the probabilities n_α, but it can be understood as a distortion of a virtual orthorhombic ground state with $n_1=1$, $n_2=n_3=n_4=0$ due to nonlinear coupling to the lattice (Fig. 3). The distorted configuration of Fig. 3 yields the real ground state shown on the bottom right of Fig. 2.

It was shown in Ref. 11 that the correct sequence of phase changes is obtained only if in addition to the two-particle interactions, the four-particle interactions are also taken into account. In the molelcular-field approximation (MFA) of the order-disorder model, the free energy F per one CH_3NH_3 group was calculated to be

$$F^*=\tfrac{1}{2}a(n_1^2+n_2^2+n_3^2+n_4^2)+b(n_1n_2+n_2n_3+n_3n_4+n_4n_1)+c(n_1n_3+n_2n_4)+d(n_1n_2n_3n_4)$$
$$+e(n_1n_2n_3+n_2n_3n_4+n_3n_4n_1+n_4n_1n_2)-kT(n_1\ln n_1+n_2\ln n_2+n_3\ln n_3+n_4\ln n_4)\ . \tag{1}$$

The analysis of the stability conditions for the disordered tetragonal high-temperature (THT) phase yielded three different symmetry-breaking fluctuation eigenvectors $\delta\eta_1$, $\delta\eta_2$, and $\delta\eta_3$ (Fig. 4), and the corresponding stability limits, respectively, transition temperatures T_1, T_2, and T_3, i.e.,

$$\begin{aligned}
&\delta\eta_1\text{:}\quad \delta n_1=-\delta n_3\ ,\quad \delta n_2=\delta n_4=0\ ,\\
&\delta\eta_2\text{:}\quad \delta n_2=-\delta n_4\ ,\quad \delta n_1=\delta n_3=0\ ,\\
&\delta\eta_3\text{:}\quad \delta n_1=\delta n_3=-\delta n_2=-\delta n_4\ ,\\
&T_1=T_2=(c-a+\tfrac{1}{16}d+\tfrac{1}{2}e)/4k\ ,\\
&T_3=(2b-c-a+\tfrac{1}{16}d+\tfrac{1}{2}e)/4k\ .
\end{aligned} \tag{2}$$

The order parameters η_1, η_2, and η_3 corresponding to the above symmetry-breaking fluctuation eigenvectors are the following linear combinations of the site-occupation probabilities n_α:

$$\begin{aligned}
&\eta_1=2n_1-2n_3\ ,\\
&\eta_2=2n_2-2n_4\ ,\\
&\eta_3=2n_1+2n_2-1=1-2n_2-2n_4\ .
\end{aligned} \tag{3}$$

The conditions $n_i\geq 0$ and $n_1+n_2+n_3+n_4=1$ implicate the following ranges for η_i:

$$\begin{aligned}
&-1\leq\eta_3\leq+1\ ,\\
&-1-\eta_3\leq\eta_1\leq+1+\eta_3\ ,\\
&-1+\eta_3\leq\eta_2\leq+1-\eta_3\ .
\end{aligned} \tag{4}$$

The different phases can be described by the equilibrium values of the above three-order parameters as follows:

$$\begin{aligned}
&\text{THT:}\quad \langle\eta_1\rangle=\langle\eta_2\rangle=\langle\eta_3\rangle=0\\
&\text{ORT:}\quad \begin{cases}\langle\eta_1\rangle\neq 0\ ,\quad \langle\eta_2\rangle=0\ ,\quad \langle\eta_3\rangle>0\\ \langle\eta_1\rangle=0\ ,\quad \langle\eta_2\rangle\neq 0\ ,\quad \langle\eta_3\rangle<0\end{cases}\\
&\text{ORT ground state:}\quad \begin{cases}\langle\eta_1\rangle=\pm 2\ ,\quad \langle\eta_2\rangle=0\ ,\quad \langle\eta_3\rangle=+1\\ \langle\eta_1\rangle=0\ ,\quad \langle\eta_2\rangle=\pm 2\ ,\quad \langle\eta_3\rangle=-1\end{cases}\\
&\text{TLT:}\quad \langle\eta_1\rangle=|\langle\eta_2\rangle|\neq 0\ ,\quad \langle\eta_3\rangle=0\\
&\text{TLT ground state:}\quad \begin{cases}\langle\eta_1\rangle=\langle\eta_2\rangle=\pm 1\\ \langle\eta_1\rangle=-\langle\eta_2\rangle=\pm 1\end{cases}\langle\eta_3\rangle=0
\end{aligned} \tag{5}$$

In these descriptions all possible domains are included. The sign of $\langle\eta_3\rangle$ in the ORT phase is a consequence of the fact that in the orthorhombic ground state the occupation probability n_α is equal to 1 for one potential well and zero for the other three. As we see in Sec. III, the model also contains an intermediate orthorhombic phase with $\langle\eta_1\rangle\neq 0$, $\langle\eta_2\rangle\neq 0$, and $\langle\eta_3\rangle\neq 0$. This phase was, however,

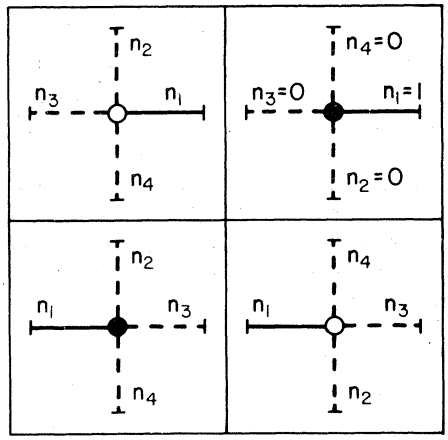

FIG. 3. Representation of the eigenvector $(n_1=1, n_2=n_3=n_4=0)$ for one of the four possible model ground states which corresponds to the frozen in ORT domain shown in Fig. 2. The projection and the assignment of the n_α are the same as in Fig. 2. The THT, ORT and TLT phases can be constructed by linear combinations of the four eigenvectors belonging to the orthorhombic model ground state.

not observed experimentally either in $(CH_3NH_3)_2CdCl_4$ or in $(CH_3NH_3)_2MnCl_4$.

In order to obtain the monoclinic ground state, a nonlinear coupling between the order parameter η_3 and the phonon coordinates δq_1 and δq_2 corresponding to the monoclinic soft modes was introduced. This takes care of the fact that the modes δq_1 and δq_2 are stable and cannot get soft as long as the corresponding site-occupation probabilities n_2+n_4 or n_1+n_3 are higher than a critical limit.[11,17] The free energy F was calculated as a function of the five order parameters η_1, η_2, η_3, q_1, and q_2 in units of kT_1 as follows:

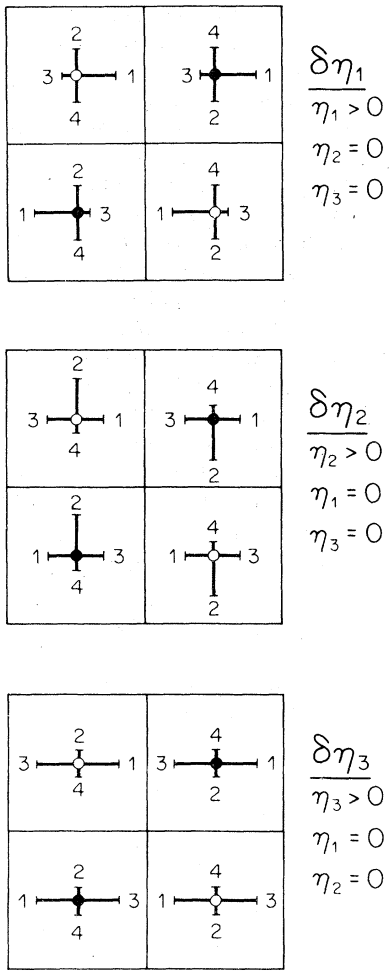

FIG. 4. Schematic representation of the eigenvectors $\delta\eta_1$, $\delta\eta_2$, and $\delta\eta_3$ according to Eq. (2) and of the corresponding order parameters according to Eq. (3).

$$F=-\tfrac{1}{4}(\eta_1^2+\eta_2^2)-\tfrac{1}{2}\tau^*\eta_3^2+\tfrac{1}{2}\delta(\eta_1^2-\eta_2^2)\eta_3+\tfrac{1}{4}\Delta(\eta_3^4-\eta_1^2\eta_3^2-\eta_2^2\eta_3^2+\eta_1^2\eta_2^2)+\frac{1}{2}\frac{f}{kT_1}(\eta_0-\eta_3)q_1^2+\frac{1}{4}\frac{g}{kT_1}q_1^4$$

$$+\frac{1}{6}\frac{h}{kT_1}q_1^6+\frac{1}{2}\frac{f}{kT_1}(\eta_0+\eta_3)q_2^2+\frac{1}{4}\frac{g}{kT_1}q_2^4+\frac{1}{6}\frac{h}{kT_1}q_2^6+\tfrac{1}{4}t^*$$

$$\times[(1+\eta_1+\eta_3)\ln(1+\eta_1+\eta_3)+(1+\eta_2-\eta_3)\ln(1+\eta_2-\eta_3)+(1-\eta_1+\eta_3)\ln(1-\eta_1+\eta_3)$$

$$+(1-\eta_2-\eta_3)\ln(1-\eta_2-\eta_3)-8\ln 2]+K\,, \tag{6}$$

where $t^*=T/T_1$, $\tau^*=T_3/T_1$, $\delta=(d+4e)/64kT_1$, and $\Delta=d/64kT_1$. For the case of $(CH_3NH_3)_2CdCl_4$, the following set of coefficients yielded the correct sequence of phase changes and the proper transition temperatures[11]: $\tau^*=0.30$, $\Delta=0.40$, $\delta=0.45$, $\eta_0=0.625$, $f:g:h=\frac{2}{3}:-1:1.25$, with $g=-kT_1$.

This set of coefficients will be used for all calculations in this paper. Figure 5 shows the temperature dependence of the order parameters and of the free energy for this set of coefficients.

A group-theoretical analysis[16] of all above phases has shown that the order-disorder model is in accordance with the symmetry of the lattice modes which condense at the transition points. The linear combinations of the Cl symmetry coordinates with the lowest frequencies are rotations of the Cl octahedra around the X, Y, and Z axes of the TLT unit cell. The rotations around the Y or X axes which condense at T_1 yield a washboardlike distortion of the layers. They transform like $\delta\eta_1$ or $\delta\eta_2$, respectively, according to the X_4^+ representation of the THT space group $I4/mmm$.[17–19] Thus a linear coupling between $\delta\eta_1$ and the corresponding lattice mode has to be taken into account. Such a coupling leads, however, only to a renormalization of the transition temperatures as shown, e.g., in Ref. 20. The mode $\delta\eta_3$ transforms

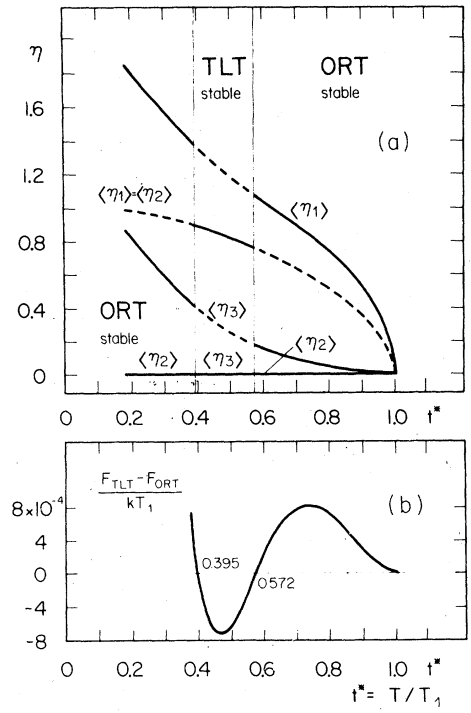

FIG. 5. Solution of the self-consistent equations for the order parameters $\langle\eta_1\rangle$, $\langle\eta_2\rangle$, and $\langle\eta_3\rangle$, of the rigid lattice model[11] for the ORT and TLT phases and the set of coefficients (τ^*, Δ, δ) given in the text. The equilibrium values of the order parameters (full lines) are plotted vs the reduced temperature t^*(a). The dashed lines correspond to unstable solutions. From the difference in the free energy of the ORT and TLT phases $(T_{\mathrm{TLT}}-F_{\mathrm{ORT}})/kT_1$ vs reduced temperature (b) one can see which of the two phases is stable for a given temperature.

according to the Γ_4^+ representation of $I4/mmm$, but there are no nonvanishing symmetry coordinates from the rest of the lattice having this symmetry. Therefore no linear coupling does exist between $\delta\eta_3$ and the octahedral matrix. A nonlinear coupling between η_3 and the monoclinic modes δq_1 and δq_2 can account for the real monoclinic ground state.

The aim of the present work is to discuss the dynamic properties of the above model in the light of the soft modes observed by Raman spectroscopy.[14] In Sec. II the dynamic properties of the four-site model are studied in a relaxation approximation. In Sec. III the orthorhombic intermediate phase $Pccn$—which is contained in the order-disorder model—is analyzed. In Sec. IV the model is extended to include the observed antiphase motion of adjacent layers.

II. DYNAMICS OF THE FOUR-SITE MODEL

Low-frequency Raman scattering[14] revealed, below 40 cm^{-1}, a temperature-dependent overdamped mode in the TLT and ORT phases. In the ORT phase the center of the signal is masked by the strong elastic peak at 0 cm^{-1}, and only the wings can be observed. On approaching the ORT-THT transition, the mode becomes so narrow that it can no longer be distinguished from the elastic peak. Thus it seems justified to use a relaxation-type equation of motion for the order-parameter dynamics.

$$-\frac{dp_i}{dt}=\Gamma_i\frac{\partial F(p_i,T)}{\partial p_i}\ , \tag{7}$$

$$p_i=\eta_1,\eta_2,\eta_3,q_1,q_2\ ,$$

$$i=1,2,3,4,5\ ,$$

where the Γ_i represent the kinetic coefficients which are not critical. Expanding the equation of motion [Eq. (7)] with respect to all order-parameter fluctuations $\delta p_i=p_i-\langle p_i\rangle$, yields

$$\delta p_i/\tau=\Gamma_i\sum_{j=1}^{5}\frac{\partial^2 F}{\partial p_i\partial p_j}\delta p_j \qquad (i=1,2,\ldots,5)\ . \tag{8}$$

The system of the five coupled equations [Eq. (8)] has five eigenvalues $1/\tau$, and the corresponding eigenvectors determine the five order-parameter fluctuations modes in all phases. By using the equilibrium values $\langle p_i\rangle$ obtained from the minimization of the free energy [Eq (6)], the eigenvalues $1/\tau$, can be obtained by diagonalizing the matrix of the coupled equations [Eq. (8)]. In the general case this matrix is not symmetric since the rows of the symmetric matrix $\partial^2F/\partial p_i\partial p_j$ are multiplied by the kinetic coefficients Γ_i which are not necessarily equal. For symmetry reasons we have

$$\Gamma_1=\Gamma_2 \quad\text{and}\quad \Gamma_4=\Gamma_5 \tag{9}$$

The "rigid-lattice" (pure order-disorder) model also yields $\Gamma_3 = \Gamma_1$. But if the coupling to the lattice is taken into account, Γ_3 is in the general case different from Γ_1 since there are no symmetry coordinates in any phase transforming like $\delta\eta_3$. In our approach we assume that the kinetic coefficients Γ_i do not show any temperature dependence.

The following schematic representations show the structure of the matrix [Eq. (8)] for the different phases. For the ORT and MLT phases only, the domains with $\langle\eta_3\rangle > 0$ are shown. The nonvanishing matrix elements are indicated by X.

$$\text{THT}\begin{pmatrix} X & & & & \\ & X & & & \\ & & X & & \\ & & & X & \\ & & & & X \end{pmatrix}$$

$$\text{ORT}\begin{pmatrix} X & & X & & \\ & X & & & \\ X & & X & & \\ & & & X & \\ & & & & X \end{pmatrix}$$

$$\text{TLT}\begin{pmatrix} X & X & X & & \\ X & X & X & & \\ X & X & X & & \\ & & & X & \\ & & & & X \end{pmatrix}$$

$$\text{MLT}\begin{pmatrix} X & & X & X & \\ & X & & & \\ X & & X & X & \\ X & & X & X & \\ & & & & X \end{pmatrix}.$$

In the tetragonal high-temperature phase THT, we have $\langle p_i\rangle = 0$. The matrix is already diagonal—i.e., there is no coupling between the five different symmetry-breaking modes—and one obtains for the eigenvalues

$$1/\tau_1 = 1/\tau_2 = \tfrac{1}{2}\Gamma_1(t^* - 1)\ ,$$
$$1/\tau_3 = \Gamma_3(t^* - \tau^*)\ , \qquad (10)$$
$$1/\tau_4 = 1/\tau_5 = \Gamma_4(f/kT_1)\eta_0\ .$$

The corresponding eigenvectors are, of course, $\delta\eta_1$, $\delta\eta_2$, $\delta\eta_3$, δq_1, and δq_2. As it can be seen from Fig. 2 the two degenerate modes $\delta\eta_1$ and $\delta\eta_2$ become soft at the Brillouin-zone (BZ) boundary[17]. Depending on the ORT domain, we look at

$$\langle\eta_1\rangle \neq 0\ ,\quad \langle\eta_2\rangle = 0\ ,\quad \langle\eta_3\rangle > 0\ ,$$

or

$$\langle\eta_1\rangle = 0\ ,\quad \langle\eta_2\rangle \neq 0\ ,\quad \langle\eta_3\rangle < 0\ ,$$

one of them condenses at T_1, where τ_1 and τ_2 diverge. τ_3 would diverge at T_3 if $T_3 > T_1$. In our case, where $\tau^* = T_3/T_1 = 0.30$, $1/\tau_3$ does not reach zero. The doubly degenerate modes δq_1 and δq_2 are not temperature dependent in our model.

Figure 6 shows the temperature dependence of the order-parameter fluctuation frequencies $1/\tau$ for all phases with $\Gamma_1 = \Gamma_2 = \Gamma_3 = kT_1/\hbar$ and $\Gamma_4(f/kT_1)\eta_0 = kT_1/\hbar$. The symmetry of the modes is given for the standard setting of axes used in the *International Tables for Crystallography*[21] for the different space groups. These axes are indicated also in Fig. 1.

In the ORT phase the two modes $\delta\eta_1$ and $\delta\eta_2$ have different relaxation times. The soft mode $\delta\eta_1$, with some admixture of $\delta\eta_3$, becomes the fully symmetric mode Γ_1^+, and shows a mean-field-type soft-mode behavior near T_1. At lower temperatures the coupling between $\delta\eta_1$ and $\delta\eta_3$ becomes stronger. The mode $\delta\eta_2$ remains a zone-boundary mode Y_3^+. Its re-

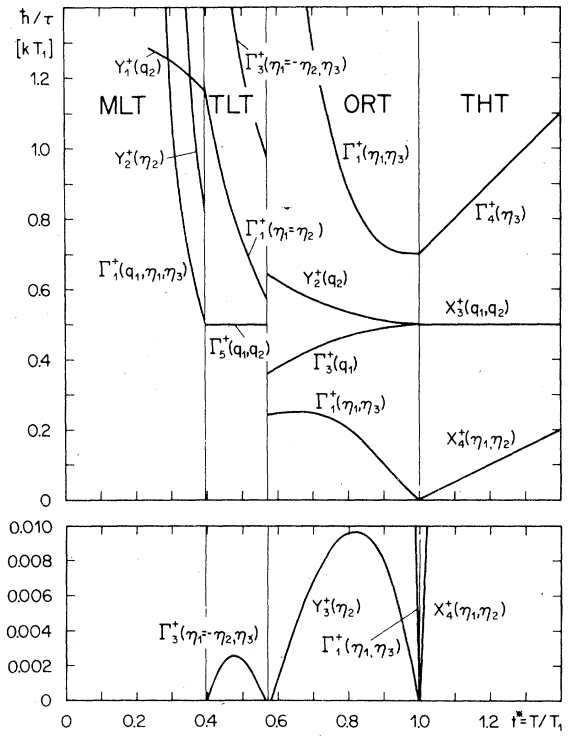

FIG. 6. Temperature dependence of the order-parameter fluctuation frequencies $1/\tau$ for all phases. At the bottom the lower part of the figure is expanded by a factor of 50 in order to display the soft modes Y_3^+ and Γ_3^+ of the ORT-TLT transition, which cannot be seen in the upper part of the figure. The kinetic coefficients Γ_i of the equation of motion were chosen as $\Gamma_1 = \Gamma_2 = \Gamma_3 = kT_1/\hbar$, $\Gamma_4 = \Gamma_5 = (kT_1/f\eta_0)(kT_1/\hbar)$.

laxation frequency $1/\tau$ is so low that the scale had to be expanded by a factor of 50 to display it. $\delta\eta_2$ is the soft mode of the ORT-TLT transition. With the expansion of the scale it became obvious that, just before reaching the TLT-phase, $1/\tau$ of this mode becomes negative, i.e., the ORT phase becomes unstable before the TLT phase is stable. Thus for a narrow temperature range an intermediate phase must appear. This intermediate phase is treated in Sec. III. The mode $\delta\eta_3$, with some admixture of $\delta\eta_1$, also has the full symmetry Γ_1^+ of the ORT phase, but it is not the soft mode. The modes δq_1 and δq_2 now have different relaxation times and show a slight temperature dependence. The coefficients $\Gamma_4=\Gamma_5$ are chosen arbitrarily, in order to show the qualitative behavior.

In the TLT phase the fully symmetric mode Γ_1^+ has the eigenvector $\delta\eta_1=\delta\eta_2, \delta\eta_3=0$. This mode is, however, not the soft mode of the ORT-TLT transition. The soft mode has the symmetry Γ_3^+ and the eigenvector $\delta\eta_1=-\delta\eta_2$ with some admixture of $\delta\eta_3$. The reason for this is that the tetragonal symmetry must be broken on going from TLT to ORT and this cannot be achieved by the Γ_1^+ mode. There is another symmetry-breaking mode Γ_3^+ at higher values of $1/\tau$. The eigenvector is very similar to the previous one $\delta\eta_1=-\delta\eta_2$, but with an admixture of $-\delta\eta_3$. This mode does not lead to the ORT phase defined in Eqs. (5) and thus cannot be the soft mode. The modes δq_1 and δq_2 are again degenerate, and show no temperature dependence.

In the MLT phase the fully symmetric mode (Γ_1^+) is a linear combination of δq_1, $\delta\eta_1$, and $\delta\eta_3$. Since the order is almost complete, we have $\delta\eta_1=\delta\eta_3$, i.e., $n_3\simeq 0, \delta n_1=-\delta n_2-\delta n_4$. The relaxation times of the modes depend not only on the coefficients $\Gamma_4=\Gamma_5$, but also depend strongly on the values of the coefficients f,g,h of Eq. (6). The value $g=-kT_1$ is at the lower boundary of the range $-kT_1>g>-10kT_1$ given in Ref. 11. This value was chosen to have at least some of the MLT modes in the range of the scale of Fig. 6.

Figure 7 shows the temperature dependence of the order-parameter fluctuation frequencies for $\Gamma_1=\Gamma_2=kT_1/\hbar$, but $\Gamma_3=kT_1/5\hbar$. All other coefficients are the same as used already for the calculation of the graphs in Fig. 6. The comparison of Figs. 6 and 7 shows that only the modes containing components of $\delta\eta_3$ are affected by reducing Γ_3 from $kT_1/\hbar$ to $kT_1/5\hbar$, i.e., in THT $\Gamma_4^+(\delta n_3)$; in ORT the two modes Γ_1^+ $(\delta\eta_1, \delta\eta_3)$: in TLT the two modes Γ_3^+ $(\delta\eta_1=-\delta\eta_2, \pm\delta\eta_3)$; and MLT $\Gamma_1^+(\delta q_1, \delta\eta_1, \delta\eta_3)$. In the ORT phase, the coupling between the $\delta\eta_1$, $\delta\eta_3$ modes became much stronger, resulting in a change in the slope of the soft Γ_1^+ mode.

The overdamped mode observed by Raman spectroscopy[14] contains components of the following symmetries: ORT: Γ_1^+, Γ_2^+; TLT: Γ_3^+, Γ_4^+. Obviously the ORT Γ_2^+ and the TLT Γ_4^+ modes are not contained in our model. An extension of the model to include these modes is given in Sec. IV.

III. INTERMEDIATE-PHASE *Pccn*

It was shown in Ref. 17 that the orthorhombic space group *Pccn* [orthorhombic low temperature (OLT)] with $Z=4$ is obtained when both $\langle\eta_1\rangle$ and $\langle\eta_2\rangle$ differ from zero. Also, $\langle\eta_3\rangle$ may differ from zero in this phase. The TLT-phase $P4_2/ncm$ is realized only if $|\langle\eta_1\rangle|=|\langle\eta_2\rangle|$ and $\langle\eta_3\rangle=0$. Thus it has to be expected that the OLT phase is stable in the temperature range around $t^*=0.6$, where the TLT as well as the ORT phases become unstable. In order to obtain the stable minima of the free energy F, one has to solve the self-consistency equations for all three-order parameters of the "rigid-lattice" model as follows:

$$\frac{\partial F}{\partial\eta_1}=-\tfrac{1}{2}\eta_1+\delta\eta_1\eta_3+\tfrac{1}{2}\Delta(-\eta_1\eta_3^2+\eta_1\eta_2^2)+\tfrac{1}{4}t^*[\ln(1+\eta_1+\eta_3)-\ln(1-\eta_1+\eta_3)]=0\,,$$

$$\frac{\partial F}{\partial\eta_2}=-\tfrac{1}{2}\eta_2-\delta\eta_2\eta_3+\tfrac{1}{2}\Delta(-\eta_2\eta_3^2+\eta_2\eta_1^2)+\tfrac{1}{4}t^*[\ln(1+\eta_2-\eta_3)-\ln(1-\eta_2-\eta_3)]=0\,, \tag{11}$$

$$\frac{\partial F}{\partial\eta_3}=-\tau^*\eta_3+\tfrac{1}{2}\delta(\eta_1^2-\eta_2^2)+\tfrac{1}{2}\Delta[2\eta_3^3-\eta_3(\eta_1^2+\eta_2^2)]+\tfrac{1}{4}t^*[\ln(1+\eta_1+\eta_3)-\ln(1+\eta_2-\eta_3)$$
$$+\ln(1-\eta_1+\eta_3)-\ln(1-\eta_2-\eta_3)]=0\,.$$

For the ORT phase where $\langle\eta_2\rangle=0$, we always have $\partial F/\partial\eta_2=0$, so that only two coupled equations have to be solved. In the TLT phase we have $\langle\eta_1\rangle=\langle\eta_2\rangle$, with $\langle\eta_3\rangle=0$, and the problem is reduced to one equation only since $\partial F/\partial\eta_3=0$, and $\partial F/\partial\eta_1=\partial F/\partial\eta_2$ for all temperatures. For the OLT phase, however, all three equations have to be solved simultaneously. The solutions are shown in Fig. 8(b). From Fig. 8(a) one can see that $1/\tau$ is now always positive, i.e., the solutions correspond to minima of the free energy. In Fig. 8(c), differences of the free energy $F_{\mathrm{ORT}}-F_{\mathrm{TLT}}$ and $F_{\mathrm{ORT}}-F_{\mathrm{OLT}}$ versus tempera-

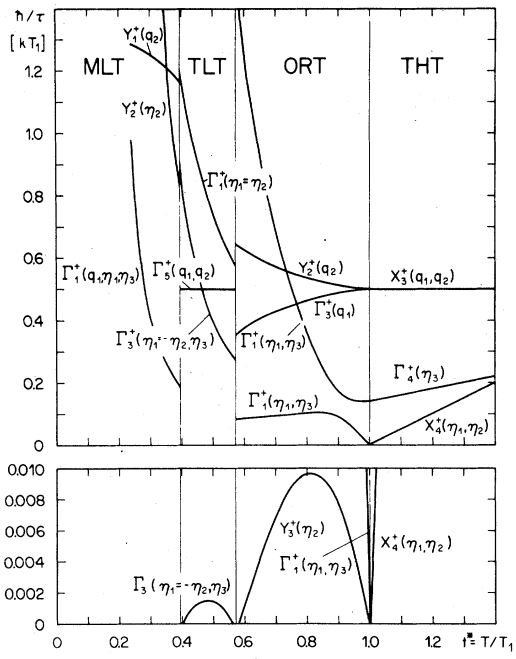

FIG. 7. Temperature dependence of the order-parameter fluctuation frequencies $1/\tau$ for all the phases. The values of the constants are the same as in Fig. 6 except for Γ_3, which now equals $kT_1/5\hbar$. The modes containing no admixture of η_3 are not affected by the change in Γ_3.

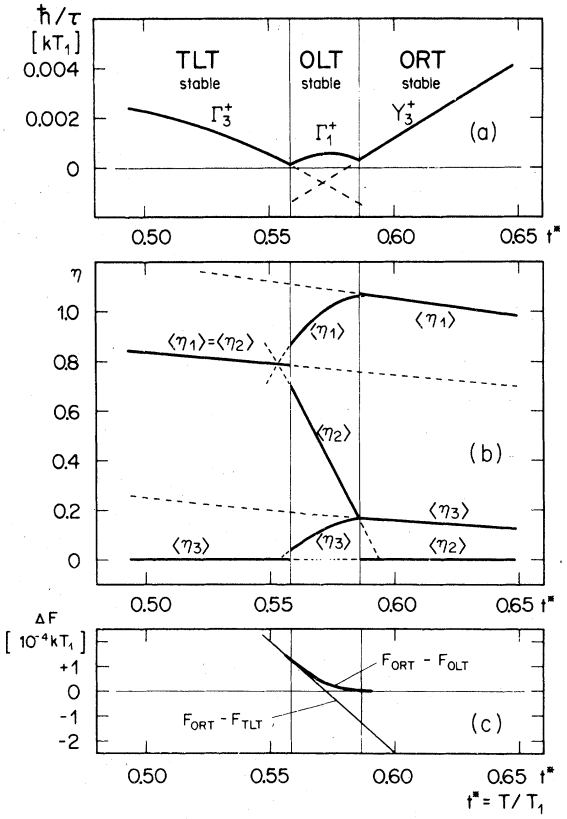

FIG. 8. Solution of the coupled Eqs. (11) for the order parameters $\langle\eta_1\rangle$, $\langle\eta_2\rangle$, and $\langle\eta_3\rangle$ for the temperature region of the ORT-TLT transition. The order-parameter fluctuation frequencies $1/\tau$ (a), the equilibrium values of the order parameters (b), and the differences in the free energies of the various phases (c), are plotted vs the reduced temperature t^*. The dashed lines (a),(b) correspond to metastable or nonstable solutions.

ture are shown for the values of the coefficients stated in the Introduction. From this, the stable solutions are obtained. The dashed lines correspond to metastable and unstable solutions.

For the "rigid-lattice" model, the phase sequence obtained in Ref. 11 was THT-ORT-TLT-ORT. Since the intermediate phase is also stable at the lowest transition temperature (TLT-ORT), the phase sequence of the model becomes

$$\text{THT}-\text{ORT}-\text{OLT}-\text{TLT}-\text{OLT}-\text{ORT}\ .$$

The OLT phase has not been observed in $(CH_3NH_3)_2CdCl_4$ and $(CH_3NH_3)_2MnCl_4$. This may be due to the fact that this phase is stable only in a temperature range which is too narrow to be observed (less than 1 K) or that it is not stable at all and is just an artifact of the above simple three-parameter (τ^*, δ, Δ) model.

With the introduction of the nonlinear coupling to the lattice modes q_1 and q_2, the coefficients f, g, h, and η_0 can be chosen so that one can reach the MLT phase directly from the TLT phase without passing through the OLT phase. We are thus left with this minor discrepancy at the ORT-TLT transition only.

IV. EXTENSION OF THE MODEL TO INCLUDE ANTIPHASE MOTION OF ADJACENT LAYERS

In order to explain the presence of the components with the symmetry Γ_2^+ (ORT) and Γ_4^+ (TLT) in the soft-mode part of the Raman spectrum, the corresponding symmetry coordinates of the two phases were analyzed. It can safely be assumed that the Cl octahedra are rather rigid and that the internal modes are at high frequencies. Thus the relevant linear combinations of symmetry coordinates are the rotations of the octahedra around the X, Y, and Z axes. The mode with the symmetry Γ_2^+ in the ORT phase ($\langle\eta_1\rangle \neq 0, \langle\eta_2\rangle = 0, \langle\eta_3\rangle > 0$) corresponds for one layer exactly to $\delta\eta_2$, but in the adjacent layers it is in antiphase compared with $\delta\eta_2$. Similarly the

mode with the symmetry Γ_4^+ in the TLT phase is a superposition of the antiphase modes of $\delta\eta_1$ and $\delta\eta_2$. Since the planewise antiphase modes are nearly equivalent to the soft modes, one can expect that they occur also at low frequencies, but do not become critical. In order to describe the antiphase modes in our order-disorder model, the free energy has to be calculated for two CH_3NH_3 groups belonging to adjacent layers. This leads to a system with eight potential wells. Figure 9 shows the new assignments of the CH_3NH_3-group orientations α ($\alpha=1,2,\ldots,8$) for eight-site model. In the molecular-field approximation, the free energy per one CH_3NH_3 group reads now as follows:

$$
\begin{aligned}
F^* = {} & \tfrac{1}{4}a'(n_1^2+n_2^2+n_3^2+n_4^2+n_5^2+n_6^2+n_7^2+n_8^2)+\tfrac{1}{2}b'(n_1n_2+n_2n_3+n_3n_4+n_4n_1+n_5n_6+n_6n_7+n_7n_8+n_8n_5) \\
& +\tfrac{1}{2}c'(n_1n_3+n_2n_4+n_5n_7+n_6n_8)+\tfrac{1}{2}a''(n_1n_5+n_2n_6+n_3n_7+n_4n_8) \\
& +\tfrac{1}{2}b''(n_1n_6+n_2n_7+n_3n_8+n_4n_5+n_1n_8+n_2n_5+n_3n_6+n_4n_7)+\tfrac{1}{2}c''(n_1n_7+n_2n_8+n_3n_5+n_4n_6) \\
& +\tfrac{1}{2}d(n_1n_2n_3n_4+n_5n_6n_7n_8) \\
& +\tfrac{1}{2}e(n_1n_2n_3+n_2n_3n_4+n_3n_4n_1+n_4n_1n_2+n_5n_6n_7+n_6n_7n_8+n_7n_8n_5+n_8n_5n_6) \\
& +\tfrac{1}{2}kT[n_1\ln(n_1)+n_2\ln(n_2)+n_3\ln(n_3)+n_4\ln(n_4)+n_5\ln(n_5)+n_6\ln(n_6)+n_7\ln(n_7)+n_8\ln(n_8)] \; . \qquad (12)
\end{aligned}
$$

The n_α are the occupation probabilities of the potential wells with the conditions

$$
\sum_{\alpha=1}^{4} n_\alpha = 1 \; , \quad \sum_{\alpha=5}^{8} n_\alpha = 1 \; , \quad 0 \le n_\alpha \le 1 \; .
$$

a', b', and c' are the coefficients of the two-particle interaction within the layer, whereas a'', b'', and c'' describe the two-particle interaction between adjacent layers. The four-particle interaction is assumed to be essentially an interaction within the layer since it describes the correlation between the four CH_3NH_3 groups surrounding one Cl octahedron. The coefficients d and e are therefore the same as used already in Eq. (1). For $n_1=n_5$, $n_2=n_6$, $n_3=n_7$, and $n_4=n_8$, the free energy of the eight-site model must be the same as the one given in Eq. (1), i.e., the two-particle coefficients of Eqs. (1) and (11) are related by $a=a'+a''$, $b=b'+b''$, and $c=c'+c''$.

The stability conditions for the disordered high-symmetry parent phase (THT: $n_\alpha=\frac{1}{4}$, $\alpha=1-8$) are obtained by diagonalizing the matrix of the second derivatives of F^* as follows:

$$
\frac{\partial^2 F^*}{\partial n_\alpha \partial n_\beta} = \frac{1}{2}
\begin{pmatrix}
A' & B' & C' & B' & A'' & B'' & C'' & B'' \\
B' & A' & B' & C' & B'' & A'' & B'' & C'' \\
C' & B' & A' & B' & C'' & B'' & A'' & B'' \\
B' & C' & B' & A' & B'' & C'' & B'' & A'' \\
A'' & B'' & C'' & B'' & A' & B' & C' & B' \\
B'' & A'' & B'' & C'' & B' & A' & B' & C' \\
C'' & B'' & A'' & B'' & C' & B' & A' & B' \\
B'' & C'' & B'' & A'' & B' & C' & B' & A'
\end{pmatrix} , \qquad (13)
$$

where $A'=a'+4kT$, $B'=b'+\frac{1}{16}d+\frac{1}{2}e$, $C'=c'+\frac{1}{16}d+\frac{1}{2}e$, and

$$
A''=a'' \; , \quad B''=b'' \; , \quad C''=c'' \; .
$$

The eigenvalues x_i of this matrix are given by

$$
\begin{aligned}
x_1 &= x_2 = a'-c'+a''-c''-\tfrac{1}{16}d-\tfrac{1}{2}e+4kT \; , \\
x_3 &= a'-2b'+c'+a''-2b''+c''-\tfrac{1}{16}d-\tfrac{1}{2}e+4kT \; , \\
x_4 &= x_5 = a'-c'-a''+c''-\tfrac{1}{16}d-\tfrac{1}{2}e+4kT \; , \\
x_6 &= a'-2b'+c'-a''+2b''-c''-\tfrac{1}{16}d-\tfrac{1}{2}e+4kT \; , \\
x_7 &= a'+2b'+c'+a''+2b''+c''+\tfrac{3}{16}d+\tfrac{3}{2}e+4kT \; , \\
x_8 &= a'+2b'+c'-a''-2b''-c''+\tfrac{3}{16}d+\tfrac{3}{2}e+4kT \; , \qquad (14)
\end{aligned}
$$

and the corresponding eigenvectors—representing deviations from the THT equilibrium-occupation probabilities— are

$$
\begin{aligned}
&\delta\eta_1: \; \delta n_1=\delta n_5=-\delta n_3=-\delta n_7, \; \delta n_{2,4,6,8}=0 \; , \\
&\delta\eta_2: \; \delta n_2=\delta n_6=-\delta n_4=-\delta n_8, \; \delta n_{1,3,5,7}=0 \; , \\
&\delta\eta_3: \; \delta n_1=\delta n_3=\delta n_5=\delta n_7=-\delta n_2=-\delta n_4=-\delta n_6=-\delta n_8 \; , \\
&\delta\eta_4: \; \delta n_1=\delta n_7=-\delta n_3=-\delta n_5, \; \delta n_{2,4,6,8}=0 \; , \\
&\delta\eta_5: \; \delta n_2=\delta n_8=-\delta n_4=-\delta n_6, \; \delta n_{1,3,5,7}=0 \; , \\
&\delta\eta_6: \; \delta n_1=\delta n_3=\delta n_6=\delta n_8=-\delta n_2=-\delta n_4=-\delta n_5=-\delta n_7 \; , \\
&\delta\eta_7: \; \delta n_\alpha=0 \; , \\
&\delta\eta_8: \; \delta n_\alpha=0 \; , \quad \alpha=1,2,\ldots,8 \; , \qquad (15)
\end{aligned}
$$

They are represented in Figs. 4 and 10. Comparing expressions (2) and (15), we see that the eigenvectors $\delta\eta_1$, $\delta\eta_2$, and $\delta\eta_3$ of the two models are identical. The new eigenvectors $\delta\eta_4$, $\delta\eta_5$, and $\delta\eta_6$ correspond to the antiphase motion of adjacent layers. Thus the model contains now the missing modes. The THT phase is stable as long as all eigenvalues x_i are positive. The stability limits T_i for the six nontrivial eigenvectors η_i are given by

$$
\begin{aligned}
T_{1,2} &= (-a + c + \tfrac{1}{16}d + \tfrac{1}{2}e)/4k \ , \\
T_3 &= (-a + 2b - c + \tfrac{1}{16}d + \tfrac{1}{2}e)/4k \ , \\
T_{4,5} &= (-a' + a'' + c' - c'' + \tfrac{1}{16}d + \tfrac{1}{2}e)/4k \ , \\
T_6 &= [-a' + a'' + 2(b' - b'') - c' + c'' \\
&\qquad + \tfrac{1}{16}d + \tfrac{1}{2}e]/4K \ .
\end{aligned}
\tag{16}
$$

$T_{1,2}$ and T_3 are the same as already given in Eq. (2). In order to have a phase transition from THT to ORT, $T_{1,2}$ must be higher than $T_{4,5}$. For the same reason T_6 must be lower than $T_{1,2}$.

The order parameters corresponding to the eigenvectors $\delta\eta_i$ can be defined as

$$
\begin{aligned}
&\eta_1 = n_1 - n_3 + n_5 - n_7 \ , \quad \eta_2 = n_2 - n_4 + n_6 - n_8 \ , \\
&\eta_3 = n_1 + n_3 + n_5 + n_7 - 1 = 1 - n_2 - n_4 - n_6 - n_8 \ , \\
&\eta_4 = n_1 - n_3 - n_5 + n_7 \ , \quad \eta_5 = n_2 - n_4 - n_6 + n_8 \ , \\
&\eta_6 = n_1 + n_3 + n_6 + n_8 - 1 = 1 - n_2 - n_4 - n_5 - n_7 \ .
\end{aligned}
\tag{17}
$$

The free energy F^* can now be expressed by the order parameters η_i, the stability limits T_i, and the coefficients Δ and δ for the four-particle interaction as already used in Eq. (6). Since there is no coupling between the monoclinic modes q_1, q_2 and the $\delta\eta_i$ in the THT, ORT, and TLT phases, the free energy has to be calculated for the order-disorder model only. In units of kT_1, the free energy is now

$$
\begin{aligned}
F = &-\tfrac{1}{4}(\eta_1^2 + \eta_2^2) - \tfrac{1}{4}\frac{T_4}{T_1}(\eta_4^2 + \eta_5^2) - \tfrac{1}{2}\frac{T_3}{T_1}\eta_3^2 - \tfrac{1}{2}\frac{T_6}{T_1}\eta_6^2 + \tfrac{1}{2}\delta[\eta_3(\eta_1^2 + \eta_4^2 - \eta_2^2 - \eta_5^2) + 2\eta_6(\eta_1\eta_4 - \eta_2\eta_5)] \\
&+ \tfrac{1}{4}\Delta[\eta_3^4 + \eta_6^4 + 2\eta_3^2\eta_6^2 - (\eta_3^2 + \eta_6^2)(\eta_1^2 + \eta_2^2 + \eta_4^2 + \eta_5^2) + (\eta_1^2 + \eta_4^2)(\eta_2^2 + \eta_5^2) + 4\eta_1\eta_2\eta_4\eta_5 - 4\eta_3\eta_6\eta_1\eta_4 - 4\eta_3\eta_6\eta_2\eta_5] \\
&+ \tfrac{1}{8}t^*[(1 + \eta_1 + \eta_4 + \eta_3 + \eta_6)\ln(1 + \eta_1 + \eta_4 + \eta_3 + \eta_6) + (1 + \eta_2 + \eta_5 - \eta_3 - \eta_6)\ln(1 + \eta_2 + \eta_5 - \eta_3 - \eta_6) \\
&+ (1 - \eta_1 - \eta_4 + \eta_3 + \eta_6)\ln(1 - \eta_1 - \eta_4 + \eta_3 + \eta_6) + (1 - \eta_2 - \eta_5 - \eta_3 - \eta_6)\ln(1 - \eta_2 - \eta_5 - \eta_3 - \eta_6) \\
&+ (1 + \eta_1 - \eta_4 + \eta_3 - \eta_6)\ln(1 + \eta_1 - \eta_4 + \eta_3 - \eta_6) + (1 + \eta_2 - \eta_5 - \eta_3 + \eta_6)\ln(1 + \eta_2 - \eta_5 - \eta_3 + \eta_6) \\
&+ (1 - \eta_1 + \eta_4 + \eta_3 - \eta_6)\ln(1 - \eta_1 + \eta_4 + \eta_3 - \eta_6) + (1 - \eta_2 + \eta_5 - \eta_3 + \eta_6)\ln(1 - \eta_2 + \eta_5 - \eta_3 + \eta_6) - 16\ln 2] + K \ .
\end{aligned}
\tag{18}
$$

The observed crystal symmetry requires that the equilibrium values $\langle\eta_4\rangle$, $\langle\eta_5\rangle$, and $\langle\eta_6\rangle$ are zero in all the phases. For this case, also, the first derivatives $\partial F/\partial\eta_4, \partial F/\partial\eta_5, \partial F/\partial\eta_6$ are always equal to zero, and we are left with the three coupled Eqs. (11) for the order parameters η_1, η_2, and η_3. This shows that the static properties of the "rigid-lattice" model remain unchanged when antiphase motion of adjacent layers is taken into account.

The dynamic matrix $\partial^2 F/\partial\eta_i\partial\eta_j$ has the following structure for any value of $\langle\eta_1\rangle, \langle\eta_2\rangle, \langle\eta_3\rangle$ if the condition $\langle\eta_4\rangle = \langle\eta_5\rangle = \langle\eta_6\rangle = 0$ is fulfilled:

$$
\frac{\partial^2 F}{\partial\eta_i\partial\eta_j} = \begin{pmatrix}
X_{11} & X_{12} & X_{13} & 0 & 0 & 0 \\
X_{21} & X_{22} & X_{23} & 0 & 0 & 0 \\
X_{31} & X_{32} & X_{33} & 0 & 0 & 0 \\
0 & 0 & 0 & X_{44} & X_{12} & X_{13} \\
0 & 0 & 0 & X_{21} & X_{55} & X_{23} \\
0 & 0 & 0 & X_{31} & X_{32} & X_{66}
\end{pmatrix} , \tag{19}
$$

where

$$
\begin{aligned}
X_{44} &= X_{11} + \frac{1 - T_4/T_1}{2} \ , \\
X_{55} &= X_{22} + \frac{1 - T_4/T_1}{2} \ , \\
X_{66} &= X_{33} + \frac{T_3 - T_6}{T_1} \ .
\end{aligned}
\tag{20}
$$

The new modes $\delta\eta_4$, $\delta\eta_5$, and $\delta\eta_6$ are coupled among each other but are not coupled to the modes $\delta\eta_1, \delta\eta_2, \delta\eta_3$. Thus the modes shown in Fig. 6 remain unchanged. The temperature dependence of all six modes is shown in Fig. 11 for $\Gamma_i = 1 (i = 1, 2, \ldots, 6)$, $T_4/T_1 = 0.8$, and $T_6/T_1 = 0.25$. The Raman active modes are represented by full lines, whereas the inactive modes are represented by dashed lines. For sake of simplicity only the modes $\delta\eta_4$, $\delta\eta_5$, and $\delta\eta_6$ are assigned in Fig. 11. One can see that the ORT mode Γ_2^+, as well as the TLT mode Γ_4^+, which is now con-

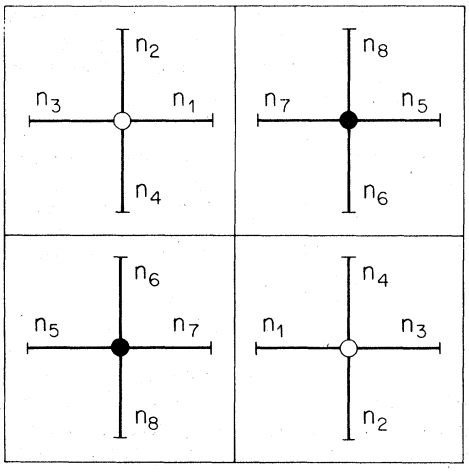

FIG. 9. Eight-site assignment of the CH_3NH_3-group orientations $\alpha(\alpha=1,2,\ldots,8)$, allowing for antiphase motions of adjacent layers as demonstrated by the experimentally observed modes Γ_2^+ of the ORT and Γ_4^+ of the TLT phases.

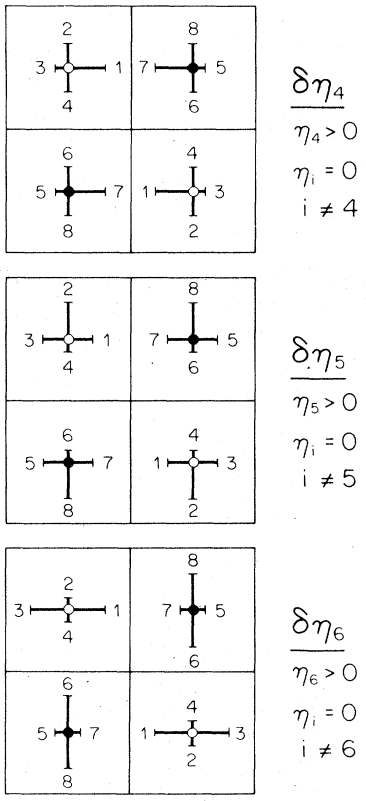

FIG. 10. Schematic representation of the eigenvectors $\delta\eta_4$, $\delta\eta_5$, and $\delta\eta_6$, which in the eight-site model occur in addition to the eigenvectors $\delta\eta_1$, $\delta\eta_2$, and $\delta\eta_3$ shown in Fig. 4.

tained in the model have similar relaxation times as the order-parameter fluctuations.

Due to lack of suitable experimental data, only a qualitative, and not a quantitative, comparison between theory and experiments can be made at this stage: The Raman data[14] give only qualitative information about the spectral evolution of the Γ_1^+ (ORT), and Γ_3^+ (TLT) soft modes. This is especially so in the ORT phase, where the signal intensity progressively decreases and the width narrows when heating the sample, so that close to the ORT-THT transition the soft mode can no longer be distinguished from the strong elastic peak located at 0 cm^{-1}. For the Γ_2^+(ORT) and Γ_4^+(TLT) modes, we know only the approximate intensity ratios to the Γ_1^+(ORT) and Γ_3^+(TLT) modes, respectively, near the TLT-ORT transition, but not the temperature dependence.

A qualitative agreement between experiment and theory for the Γ_1^+(ORT) and Γ_3^+(TLT) modes is reached by assuming that the very low-frequency Γ_3^+(TLT) mode is hidden in the strong elastic peak at

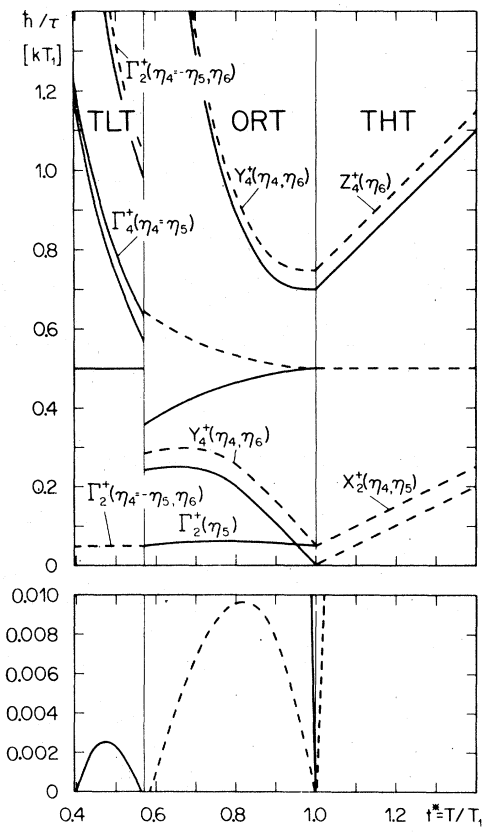

FIG. 11. Temperature dependence of the order-parameter fluctuation frequencies $1/\tau$ for the eight-site model. Only the modes which are not shown in Fig. 6 are assigned. The full lines indicate the Raman active modes, whereas the dashed lines correspond to inactive modes.

0 cm^{-1}, so that only the Γ_3^+(TLT) mode, which does not become soft, is observed. A crucial test for our theory would be a measurement of the temperature dependence of the Γ_2^+(ORT) mode which, according to Fig. 11, should not depend on temperature.

V. CONCLUSIONS

From the above results the following conclusions can be made:

(i) The soft-order parameter fluctuation modes observed in the low-frequency Raman spectra[14] can be described by a simple orientational order-disorder model, where the CH_3NH_3 groups move between four potential wells. The same model is also capable of describing the static properties of the various structural phases occuring in the pseudo-two-dimensional-layer structure compounds $(CH_3NH_3)_2CdCl_4$ and $(CH_3NH_3)_2MnCl_4$.

(ii) The nonlinear coupling of the motion of the CH_3NH_3 groups with the $CdCl_4$ octahedral matrix is not essential in the high-temperature phases (THT,ORT,TLT), but is absolutely necessary to describe the monoclinic ground state.

(iii) To explain the observed Γ_2^+ mode in the ORT and the Γ_4^+ mode in the TLT phases, the planewise antiphase motion of the CH_3NH_3 groups is included in the model. If the interlayer coupling is assumed to be much weaker than the intralayer coupling, similar fluctuation frequencies for the planewise antiphase modes are obtained as for the planewise "in-phase" modes corresponding to the condensing order-parameter modes for the four-site model.

ACKNOWLEDGMENT

This work was supported by the Swiss National Science Foundation and by the Research Community of Slovenia.

[1]R. Kind and J. Roos, Phys. Rev. B 13, 45 (1976).
[2]G. Chapuis, H. Arend, and R. Kind, Phys. Status Solidi A 31, 449 (1975).
[3]G. Chapuis, R. Kind, and H. Arend, Phys. Status Solidi A 36, 285 (1976).
[4]G. Heger, D. Mullen and K. Knorr, Phys. Status Solidi A 31, 455 (1975).
[5]G. Heger, D. Mullen, and K. Knorr, Phys. Status Solidi A 35, 627 (1976).
[6]N. Lehner, K. Strobel, R. Geick, and G. Heger, J. Phys. C 8, 4096 (1975).
[7]D. Brinkmann, U. Walther, and H. Arend, Solid State Commun. 18, 1307 (1976).
[8]R. Blinc, M. Burgar, B. Lozar, J. Seliger, J. Slak, V. Rutar, H. Arend, and R. Kind, J. Chem. Phys. 66, 278 (1977).
[9]J. Seliger, R. Blinc, R. Kind, and H. Arend, Z. Phys. B 25, 189 (1976).
[10]A. Levstik, C. Filipic, R. Blinc, H. Arend, and R. Kind, Solid State Commun. 20, 127 (1976).
[11]R. Blinc, B. Žekš, and R. Kind, Phys. Rev. B 17, 3409 (1978).
[12]H. Arend, R. Hofmann, and F. Waldner, Solid State Commun. 13, 1629 (1973).
[13]K. Knorr, I. R. Jahn, and G. Heger, Solid State Commun. 15, 231 (1974).
[14]M. Couzi, A. Daoud, and R. Perret, Phys. Status Solidi A 36, 285 (1976).
[15]I. A. Oxton and O. Knop, J. Mol. Structure 37, 59 (1977).
[16]R. Geick and K. Strobel, J. Phys. C 12, 27 (1979).
[17]R. Kind, Phys. Status Solidi A 44, 661 (1977).
[18]J. Petzelt, J. Phys. Chem. Solids 36, 1005 (1975).
[19]R. Geick and K. Strobel, J. Phys. C 10, 4221 (1977).
[20]R. Blinc and B. Žekš, in *Soft Modes in Ferroelectrics and Antiferroelectrics, Selected Topics in Solid State Physics*, edited by P. Wohlfahrt, (North-Holland, Amsterdam, 1974), Vol. 13, p. 169.
[21]*International Tables for Crystallography*, (Kynoch, Birmingham, 1969).